

Study of Stress Induced Failure of the Blood-gas Barrier and the Epithelial-epithelial Cells Connections of the Lung of the Domestic Fowl, *Gallus gallus* Variant *Domesticus* after Vascular Perfusion

John N. Maina¹ and Sikiru A. Jimoh²

¹Department of Zoology, University of Johannesburg, Johannesburg, South Africa. ²School of Anatomical Sciences, University of the Witwatersrand, Johannesburg, South Africa.

ABSTRACT: Complete blood-gas barrier breaks (BGBBs) and epithelial-epithelial cells connections breaks (E-ECCBs) were enumerated in the lungs of free range chickens, *Gallus gallus* variant *domesticus* after vascular perfusion at different pressures. The E-ECCBs surpassed the BGBBs by a factor of ~2. This showed that the former parts of the gas exchange tissue were structurally weaker or more vulnerable to failure than the latter. The differences in the numbers of BGBBs and E-ECCBs in the different regions of the lung supplied with blood by the 4 main branches of the pulmonary artery (PA) corresponded with the diameters of the blood vessels, the angles at which they bifurcated from the PA, and the positions along the PA where they branched off. Most of the BGBBs and the E-ECCBs occurred in the regions supplied by the accessory- and the caudomedial branches: the former is the narrowest branch and the first blood vessel to separate from the PA while the latter is the most direct extension of the PA and is the widest. The E-ECCBs appeared to separate and fail from tensing of the blood capillary walls, as the perfusion- and intramural pressures increased. Compared to the mammalian lungs on which data are available, i.e., those of the rabbit, the dog, and the horse, the blood-gas barrier of the lung of free range chickens appears to be substantially stronger for its thinness.

KEY WORDS: bird, lung, blood-gas barrier, perfusion, structural failure

CITATION: Maina and Jimoh. Study of Stress Induced Failure of the Blood-gas Barrier and the Epithelial-epithelial Cells Connections of the Lung of the Domestic Fowl, *Gallus gallus* Variant *Domesticus* after Vascular Perfusion. *Biomedical Engineering and Computational Biology* 2013;5:77–88 doi:10.4137/BECB.S12988.

TYPE: Original Research

FUNDING: This work was funded by the National Research Foundation (NRF) of South Africa.

COMPETING INTERESTS: Authors disclose no potential conflicts of interest.

COPYRIGHT: © the authors, publisher and licensee Libertas Academica Limited. This is an open-access article distributed under the terms of the Creative Commons CC-BY-NC 3.0 License.

CORRESPONDENCE: jmaina@uj.ac.za

Introduction

Among vertebrates, the avian respiratory apparatus, the lung-air sac system, is structurally and functionally exceptional. It is separated into air sacs, which serve as mechanical ventilators, and the lung, which functions as the gas exchanger.^{1–3} The lungs are firmly attached to the vertebral column and the ribs and the air sacs extensively disseminate in the coelomic cavity, where they pneumatize bones, and in some species, terminate subcutaneously. One of the astonishing aspects of the structural design of the avian lung is its overall strength, particularly that of the air capillaries (ACs) and the blood capillaries (BCs), which are the minuscule terminal respiratory units that range in diameter from 3 to 20 μm .^{4,5} In contrast to the mammalian lung, which considerably collapses when punctured or

removed from the body, the avian lung very much maintains its shape and size under the same conditions. About 3 decades ago, Macklem et al⁶ showed that ACs are astoundingly strong for their minuscule size, while Powell et al⁷ observed that BCs did not distend after blood flow to one lung was doubled. More recently, in the white leghorn breed of chickens, Watson et al⁸ demonstrated that when the pressure inside the BCs was increased from 0 to 2.5 kPa, the diameter of the BCs increased by only 13% and increasing the pressure outside them (BCs) relative to that inside to 3.5 kPa did not change their diameters. In comparison, for equal pressure changes in the lungs of dogs and cats, the mean diameters of the BCs increased by ~125% and ~128% respectively, and at a higher pressure level (3.5 kPa) the BCs totally collapsed.



It is paradoxical that while in a bird lung the blood-gas barrier (BGB) is ~3 times thinner compared to that of a lung of a mammal of equivalent body mass,^{9–11} it tolerates relatively higher blood pressures¹² that are generated by large hearts¹³ with large stroke volumes.¹⁴ The means and mechanisms by which the BGB of the avian lung acquires and sustains its strength are unclear.^{3,8,11,15} Failure of the BGB and the epithelial-epithelial cell connections (E-ECCs) in the different vascular territories of the lung of the free range chickens (*Gallus gallus* variant *domesticus*) domestic fowl under different exercise intensities were previously reported by Maina and Jimoh¹⁶: it was noted that BGB breaks (BGBBs) occurred even in resting birds. The numbers of BGBBs and epithelial-epithelial cell connections breaks (E-ECCBs) increased with the intensity of exercise, and in all cases the latter surpassed the former. In the rabbit-, the dog-, and the horse lungs, the BGB fails at transmural pressures of respectively ~5, ~10, and ~14 kPa^{15,17–20}: equivalent data in birds are lacking. In this study, in an attempt to explain how the thinner avian pulmonary BGB copes with high blood pressures,¹² albeit the designs of the BGB in the bronchioalveolar (mammalian)- and parabronchial (avian) lungs being similar,^{8,10,11,21} the numbers of complete BGBBs and E-ECCBs were counted after experimental perfusion of the lungs of free range chickens at different head pressures.

Materials and Methods

Chickens. The University of the Witwatersrand's Animal Ethics Screening Committee approved this study (Clearance Number 2007/53/01). 48 mature free-range mixed breed of chickens, *Gallus gallus* variant *domesticus* which weighed between 1,392 and 2,838 g (\pm SD 409.23) were procured from a reliable breeder and kept in a holding unit of the Central Animal Service (CAS) facility for 3 weeks to acclimatize and for their health to be properly assessed. The unit was well-ventilated, the temperature was maintained at 22°C, and the chickens were exposed to 12-hour light and 12-hour darkness. They were fed on commercial food ration and occasional green vegetables. Water was provided ad libitum.

Preparation of the chickens for the experiments. The chickens were injected with 2.5 cm³ heparin (1000 IU) through

the left brachial vein, which was allowed to circulate in blood for 10 minutes. Thereafter, they were euthanized by injection with 5 cm³ of thiopentone sodium (25 mg/cm⁻³) through the right brachial vein. With the chicken lying in a supine position, the heart was accessed by cutting the ribs and removing the sternum together with the attached flight muscles. The pericardial sac was opened and the fat tissue surrounding the root of the pulmonary trunk removed up to where the blood vessel bifurcated into right- and left pulmonary arteries (PA). Cuts were made on the tips of the right and left ventricles, allowing access to the right and left ventricles. An inflow tube was inserted through the right atrioventricular valve to cannulate the pulmonary trunk and an outflow one was pushed past the left atrioventricular valve into the left atrium. The tubes were then held in place by ligature. The perfusion pressures were adjusted with manometers. The pulmonary circulation was perfused using warm (40°C) phosphate buffered saline (PBS) for 20 minutes, starting at an inflow pressure of 1.18 kPa and an outflow one of 0.69 kPa (Table 1): this created an intramural pressure of 0.94 kPa. Owing to technical difficulties of cannulating a pulmonary blood capillary and directly determining the intramural pressure within, the mean of the inflow pressure (i.e., the pressure in the PA) and the outflow pressure (i.e., the pressure in the pulmonary vein) was taken to be the average intramural capillary blood pressure, the accepted procedure in studies of the mammalian lung.^{22,23} In a pilot study, the intramural pressure of 0.94 kPa was shown to initially cause complete failure of the BGB. The perfusion pressures were subsequently increased by 49 units up to the highest inflow pressure of 3.63 kPa and an outflow one of 3.14 kPa (Table 1). After perfusion with PBS was completed, the lung was fixed by perfusion with warm (40°C) 2.5% glutaraldehyde buffered in phosphate solution (pH 7.4) for 10 minutes. The lungs were then dissected out of their attachments to the vertebral column and the ribs and post-fixed by immersion in the same fixative and stored at 4°C before sampling and processing the tissues for light- and transmission electron microscopy.

Sampling of the lung. The right lung was divided into the vascular regions, which are supplied, by the 4 branches of the PA. Transverse slices were cut along the costal sulci and the

Table 1. Perfusion pressure setting.

EXPERIMENT NUMBER	NUMBER OF BIRDS	INFLOW PRESSURE (kPa)	OUTFLOW PRESSURE (kPa)	INTRAMURAL PRESSURE* (kPa)
1	8	1.18	0.69	0.94
2	8	1.67	1.18	1.43
3	8	2.16	1.67	1.92
4	8	2.65	2.16	2.41
5	8	3.14	2.65	2.90
6	8	3.63	3.14	3.39

*The mean pulmonary capillary intramural pressure was calculated as the average of the inflow pressure (presumed pressure in the pulmonary artery) and the outflow pressure (presumed pressure in the pulmonary vein).^{22,23}

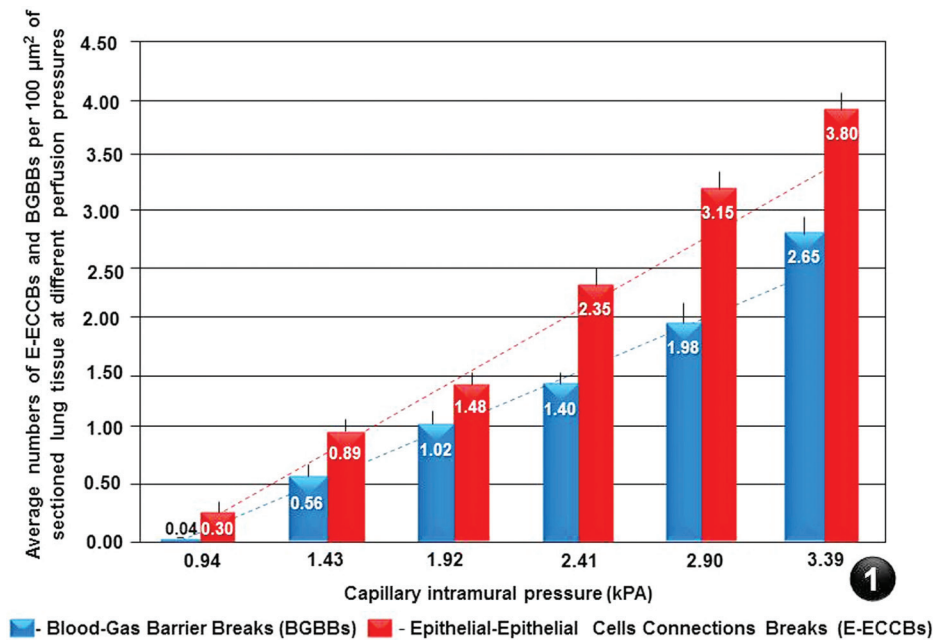


Figure 1. Relative numbers of blood-gas barrier breaks (BGGBs) and the epithelial-epithelial cells connections breaks (E-ECCs). At all perfusion pressures, the numbers of E-ECCBs surpassed the BGGBs and with increasing perfusion pressures, the E-ECCBs increased at a higher rate compared to the BGGBs. Bars: \pm SE of the mean.

slices divided into upper and lower halves along the horizontal plane followed by the primary bronchus. An acetate paper with a quadratic lattice grid with numbered squares was placed on the surface of the slices and 4 samples taken from sites corresponding to random numbers that were generated from a computer (GraphPad Software®). The samples were processed for light, transmission and scanning electron microscopy by the standard laboratory techniques. Semithinepon embedded sections ($0.3 \mu\text{m}$) were stained with toluidine blue and the numbers of complete BGGBs and E-ECCBs were counted at a final light microscope magnification of $1,000\times$ [$\times 100$ objective (oil objective) and $\times 10$ eyepiece] in randomly selected areas of $100 \mu\text{m}^2$ of sectioned lung tissues perfused at different head pressures that ranged from 0.94 kPa to 3.39 kPa . Ultrathin sections were cut and viewed on a JEOL 100S transmission electron microscope other tissues critical point, dried and sputter-coated with gold-palladium complex and viewed on a JEOL scanning electron microscope (JEOL SEM840) to determine the processes and mechanisms of BGB- and E-ECCs failures.

Statistical analysis. After ascertaining that the data were normally distributed, a Student's-t test was performed to compare the numbers of BGGBs and the E-ECCBs between the different regions of the lung supplied with blood by the 4 main branches of the PA and between different perfusion pressures. The level of significance was set at $P = 0.05$.

Results

Numbers of complete BGB- and E-ECCs breaks. The E-ECCBs- and the BGGBs increased with increasing

perfusion (intramural) pressures (Fig. 1): the rate of failure of the former sites increased at a higher rate than that of the later (Fig. 1). This showed that compared to the BGB, the E-ECCs are structurally weaker and/or more vulnerable to structural failure.

Differences between the BGB- and the E-ECCs breaks. For comparison, the numbers of BGB and E-ECC breaks in the areas supplied with blood by the 4 branches of the PA and the total number of breaks in the particular area of the lung were expressed as percentages (Fig. 2). This indicates the most frequent type of break and how the 2 types of breaks compare at different perfusion pressures. At the lowest intramural pressure of 0.94 kPa , the number of E-ECCBs in the 4 regions exceeded those of the BGB by more than 50% and no BGGBs occurred in the area supplied by the cranial branch of the PA. At the capillary intramural pressure of 1.43 kPa , compared to the preceding intramural pressure (0.94 kPa), notable differences occurred between the numbers of E-ECCBs and those of the BGB in the different regions of the lung: the number of E-ECCBs in the cranial region was 59% while the relative number of E-ECCBs in the area supplied by the caudomedial branch was only 5%. At the intramural pressure of 1.92 kPa , the relative numbers of the E-ECCBs in all the vascular regions ranged from 22 to 35% while the intramural pressure of 2.41 kPa and above, and the relative numbers of the E-ECCBs ranged from 28 to 42%.

Comparison of the BGB breaks in different regions of the lung. At the lowest intramural pressure (0.94 kPa), no BGGBs occurred in the part of the lung supplied by the cranial branch of the PA (Fig. 3); the region supplied by the

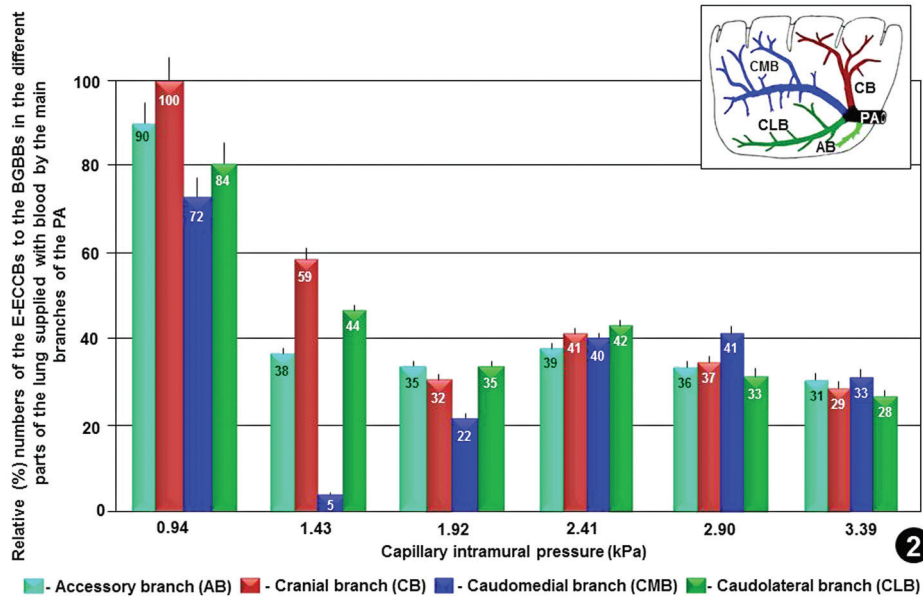


Figure 2. Relative (percentage) numbers of epithelial-epithelial cells connections breaks (E-ECCBs) and blood-gas barrier breaks (BGBBs) in the different parts of the lung supplied with blood by the 4 main branches of the pulmonary artery (PA). At the lowest intramural pressure (0.94 kPa), more than 50% of the breaks were the E-ECCs and no BGBBs occurred in the area supplied by the cranial branch; at the perfusion pressure of 1.43 kPa, the area supplied by the cranial branch had the highest number of E-ECCBs (59%) while the region supplied by the caudomedial branch had the lowest number (5%); at the intramural pressure of 1.92 kPa, the caudomedial branch had the lowest percentage number of E-ECCBs (22%) while in the other vascular territories they ranged from 32% and 35%. Above the intramural pressure of 2.41 kPa, the percentage differences between the E-ECCBs and the BGBBs ranged between 28% and 42%. Bars: \pm SE of means. Insert: Sketch of the lung showing the main branches of the PA. **Abbreviations:** AB, accessory branch; CB, cranial branch; CMB, caudomedial branch; CLB, caudolateral branch.

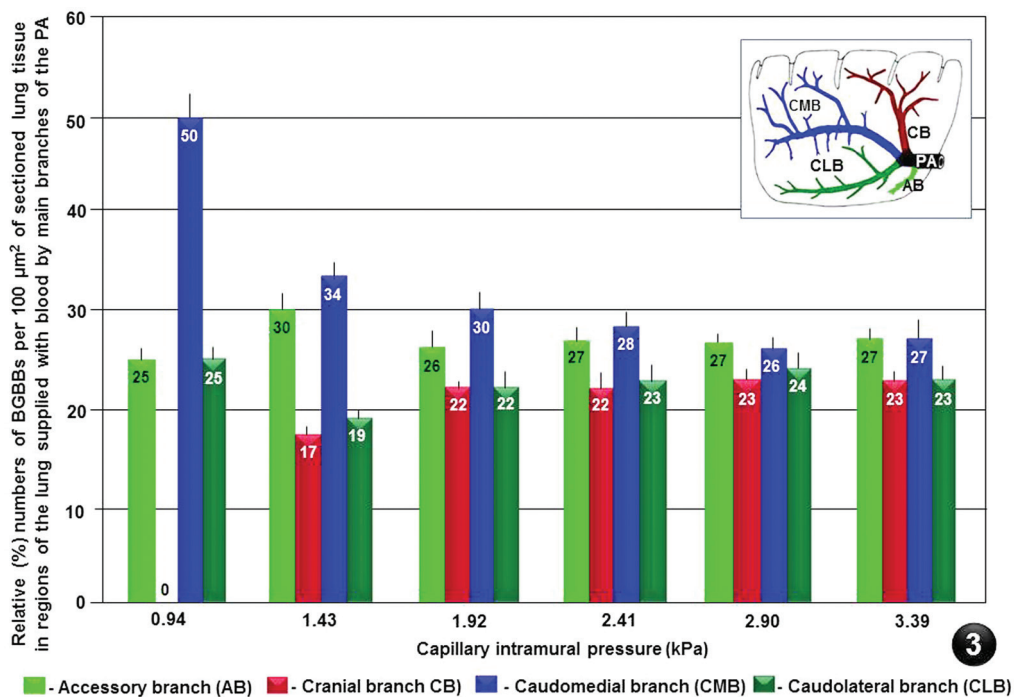


Figure 3. Relative (%) numbers of blood-gas barrier breaks (BGBBs) per 100 μm^2 of sectioned lung tissue in regions of the lung supplied with blood by the four main branches of the pulmonary artery (PA) perfused at different pressures. Most of the BGBBs occurred in the regions of the lung supplied by the accessory- and the caudomedial branches of the PA. At the intramural pressure of 0.94 kPa, no BGBBs occurred in the part of the lung supplied by the cranial branch of the PA. Bars: \pm SE of means. Insert: Sketch of the lung showing the main branches of the pulmonary artery (PA). **Abbreviations:** AB, accessory branch; CB, cranial branch; CMB, caudomedial branch; CLB, caudolateral branch.

caudomedial branch of the PA accounted for 50% of the total number of failures while the areas supplied by the accessory- and the caudolateral branches accounted for 25% each. At the intramural pressure of 1.43 kPa, the areas supplied by the accessory- and the caudomedial branches of the PA had most BGGBs. These areas accounted for 30% and 34% of the total number of BGGBs in their respective parts of the lung compared to 17% and 19% in the areas respectively supplied by the cranial- and the caudolateral branches of the PA. At the intramural pressure of 1.92 kPa and higher, each of the areas supplied by the 4 branches of the PA contributed between 22% and 30%: the accessory- and the caudomedial regions had the most breaks.

At the lowest perfusion pressure of 0.95 kPa (Fig. 3), statistically significant differences ($P < 0.001$) occurred between the number of BGGBs in the part supplied by the caudomedial branch of the PA and those supplied by the accessory- and the caudolateral branches; at a pressure of 1.43 kPa, significant differences ($P < 0.001$) occurred between the accessory- and the caudomedial branches compared to the cranial- and the caudolateral branches; at a perfusion pressure of 1.92 kPa and above, although the numbers of E-ECCBs in the areas supplied by the accessory- and caudomedial branches were more than those supplied by the cranial- and the caudolateral branches, the differences were not statistically significant ($P > 0.05$).

Comparison of E-ECCBs breaks in the different regions of the lung. At the lowest intramural pressure of 0.94 kPa, the highest number of E-ECCBs (31%) occurred in the area of the lung supplied by the accessory branch of the PA (Fig. 4) while the lowest number (21%) occurred in the part supplied by the caudolateral branch of the PA; the breaks in the areas supplied by the cranial- and the caudomedial branches contributed 24% each. At the intramural pressures of 1.43 kPa, the region supplied by the accessory branch had most breaks (31%) while the lowest value (21%) occurred in the area supplied by the caudolateral branch; the areas supplied by the cranial- and the caudomedial branches of the PA contributed 26% and 22% each. At the intramural pressure of 1.92 kPa and higher, the areas supplied by the accessory- and caudomedial branches contributed between 22 and 28%, while for those supplied by the cranial- and the caudolateral branches of the PA, the values ranged from 22 and 24%.

At the perfusion pressure of 0.95 kPa (Fig. 3), a statistically significant difference ($P < 0.001$) occurred between the number of E-ECCBs in the part of the lung supplied by the accessory branch of the PA compared to those supplied by the cranial-, the caudomedial-, and the caudolateral branches of the PA; under the perfusion pressure of 1.43 kPa, a significant difference ($P < 0.001$) occurred between the number of E-ECCBs in the accessory branch and the caudomedial- and the caudolateral branches of the PA; at the perfusion

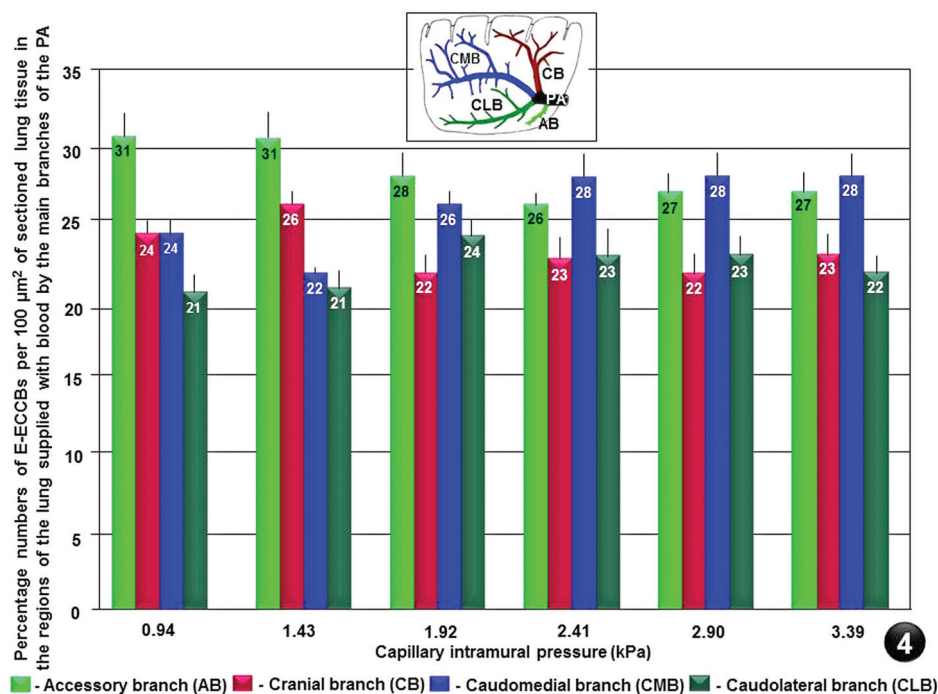


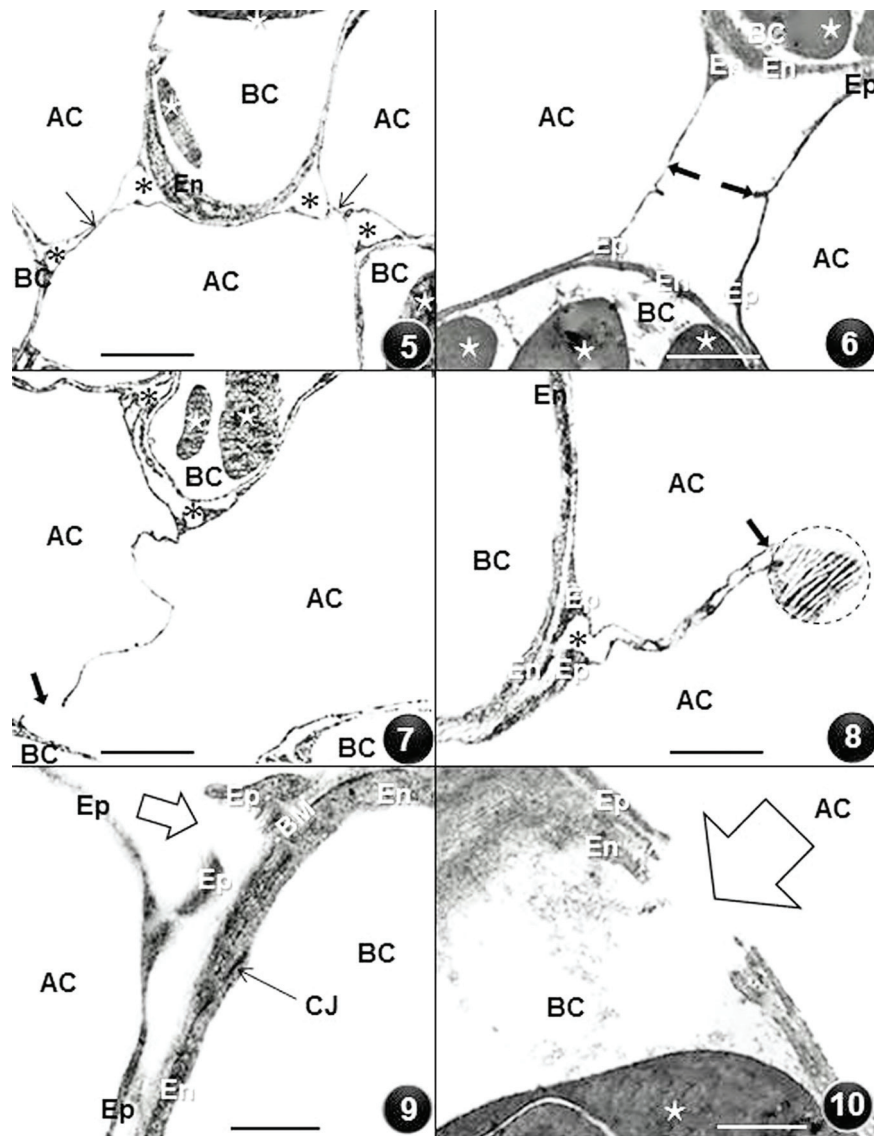
Figure 4. Percentage numbers of epithelial-epithelial cells connections breaks (E-ECCBs) per $100 \mu\text{m}^2$ of sectioned lung tissue in the regions of the lung supplied with blood by the four main branches of the pulmonary artery (PA) perfused at different pressures. At intramural pressures of 0.94, 1.43, and 1.92 kPa, the area supplied by the accessory branch had the highest numbers of E-ECCBs while above the intramural pressure of 2.41 kPa, the area supplied by the caudomedial branch had the greatest number of breaks. Bars: \pm SE of means. Insert: Sketch of the lung showing the main branches of the pulmonary artery (PA).

Abbreviations: AB, accessory branch; CB, cranial branch; CMB, caudomedial branch; CLB, caudolateral branch.

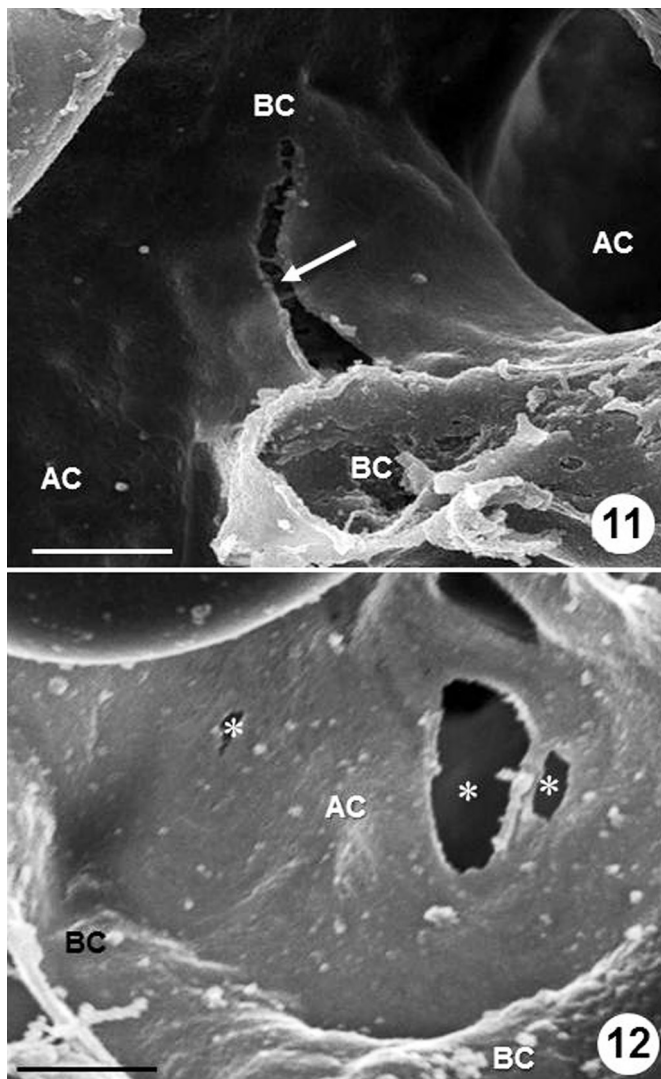
pressure of 1.93 kPa and above, the areas supplied with blood by the accessory- and the caudomedial branches of the PA had the highest numbers of E-ECCBs compared to those supplied by the cranial and the caudolateral branches of the PA, but the differences were not statistically significant ($P > 0.05$).

Mechanisms of structural failures of the E-ECCs- and the BGB breaks. Starting from the parts where they connected to the BCs, the epithelial cells separated with increasing

capillary intramural pressure (Figs. 5–9); this appeared to be caused by increased tension on the blood capillary wall. At higher perfusion pressures, BGBBs displayed jagged edges (Fig. 10), a feature that suggested forceful tearing, as the BGB resisted increasing intramural pressure up to a critical point, weakened, and then failed (Fig. 11). The failure of the E-ECCs started as discrete perforations, which progressively joined to form larger failure sites (Fig. 12). The mechanisms



Figures 5–10. Failures of the blood-gas barrier and the epithelial-epithelial cells connections. **Figure 5.** 3 blood capillaries (BC) two of which contain red blood cells (stars). The blood capillaries are connected by epithelial-epithelial cell connections (arrows), which also separate the three air capillaries (AC). En, endothelial cell; asterisks, areas where the epithelial cells have separated. Perfusion pressure 0.94 kPa. Scale bar, 2 μm . **Figure 6.** Complete separation of epithelial cells (Ep) (arrows) which connect blood capillaries (BC) while separating air capillaries (AC). En, endothelial cells; Stars, red blood cells. Perfusion pressure 0.94 kPa. Scale bar, 2 μm . **Figure 7.** Complete break of an epithelial-epithelial cells connection (arrow). Asterisks, areas where epithelial cells have separated; AC, air capillaries; BC, blood capillaries; stars, red blood cells. Perfusion pressure 1.43 kPa. Scale bar 2 μm . **Figure 8.** Separation (asterisk) and failure (arrow) of the epithelial-epithelial cells connections. BC, blood capillary; AC, air capillary; Ep, epithelial cell; En, endothelial cells. The free end of the broken epithelial-epithelial cells connection (arrow) has coiled to form a globular structure (dashed circle) which may contain congealed blood plasma. Perfusion pressure 1.43 kPa. Scale bar, 0.5 μm . **Figure 9.** Complete break of an epithelial cell (Ep) (arrow) which is separated from the endothelial cell (En) by a basement membrane (BM). CJ, cell (endothelial) junction; AC, air capillary; BC, blood capillary. Perfusion pressure 2.90 kPa. Scale bar, 0.5 μm . **Figure 10.** A red blood cell (star) contained in a blood capillary (BC) seen close to a blood-gas barrier perfusion-induced failure (arrow). Perfusion pressure 2.90 kPa. AC, air capillary, En, endothelial cell; Ep, epithelial cell. Scale bar, 0.5 μm .



Figures 11–12. Scanning electron micrographs showing areas of failures of the blood-gas barrier (the blood capillary wall) (arrow) (**Figure 11**) and that of the epithelial-epithelial cells connections (asterisks) (**Figure 12**). BC, blood capillary; AC, air capillary. Both preparations occurred under a perfusion pressure of 2.41 kPa. Scale bars, 10 μ m.

and progressions of failures of the BGB and the E-ECCs are illustrated in Figure 13: the epithelial cells failed as the intramural pressure increased, probably from accumulation of initially blood plasma and then blood on the weakening and then failure of the endothelial cell and the basement membrane.

Discussion

Although natural- and artificial structures are comprised of completely different materials, they contend with similar physical forces. In human engineering, failure expresses a loss of load-carrying capacity through damage or deformation of a component, a member, or the entire structure after overloading or working beyond its greatest load-bearing capacity or strength threshold.^{24,25} Li et al²⁶ observed that like for most machines, with time, the components of the body fail from

disease conditions and mechanical insult or normal wear and tear may induce tissue deterioration. The respiratory- and the cardiovascular systems, which are respectively charged with acquiring and distributing oxygen in the body, are continually mechanically active organs/systems. It is amazing that a person who lives to average life expectancy experiences ~5 billion heart beats and the lung is ventilated ~700 million times! During strenuous exercise, when oxygen demand is high, the heart and lungs tolerate inordinate stress and strain.^{27–29} For example, in the horse, at maximum exercise on a treadmill, the stroke volume increases by as much 41% compared to the resting value and the cardiac output increases six-fold;³⁰ in the marabou stork, *Leptoptiloscrumeniferus*, oxygen consumption (VO_2) and heart rate correlate directly,³¹ and, in an exercising pigeon, the heart rate increases 3 to 4 times from rest.³² Passively (e.g., lung) and actively dynamic (e.g., heart) organs experience recurring and nonlinear deformations throughout their working life: they display complex mechanical properties and exceptional tissue and cell organizations.³³ In the air-breathing vertebrates, survival depends on the mechanical integrity of the extremely thin and ostensibly delicate pulmonary BGB that separates air and blood, permitting oxygen and carbon dioxide to exchange by physical diffusion. During the last 3 decades, various investigators have shown that cardiopulmonary mechanics continuously challenge the integrity of the adaptively thin BGB.^{15,17,34,35} In the true sense of the word, the BGB is a ‘life-line’. Explicating the basis of the strength of the BGB and why, when, and how it fails under conditions like exercise, disease, and pathology is of particular interest to morphologists and physiologists, and is of practical importance to clinicians.

In the chicken lung, the PA gives off 4 branches that supply the different parts of the lung^{36–38}: while some of the areas overlap, the blood vessels themselves do not anastomose.³⁷ From hydrodynamic principles, the blood flow and the pressures in the different branches should correlate with structural features like the branching angles, the points along the PA where branching occurs, and the internal diameters of the branches. Overall, the absolute and the relative numbers of the E-ECCBs- and the BGGBs were higher in the areas supplied by the accessory- and the caudomedial branches of the PA, a pattern of failure which corresponded with that reported by Maina and Jimoh,¹⁶ after exercising chickens on a treadmill. While this may indicate inherent structural weakness and/or vulnerability of the E-ECCs to failure, it may also be explained by the pressures existing in the vascular branches. The caudomedial branch of the PA is the widest (2.2 mm) and is the direct continuation of the PA (branching angle 17°) while the accessory branch is the narrowest (0.8 mm), the first main blood vessel to bifurcate from the PA, and branches from the PA at an angle of 44 degrees.^{16,38} Blood flow in the different vascular territories of the lung and local control at the parabronchial level depends on regional and local changes in vascular resistance.³⁹ In the chicken lung, presence of smooth muscles in the interparabronchial vessels may control blood flow along a parabronchus.³⁷

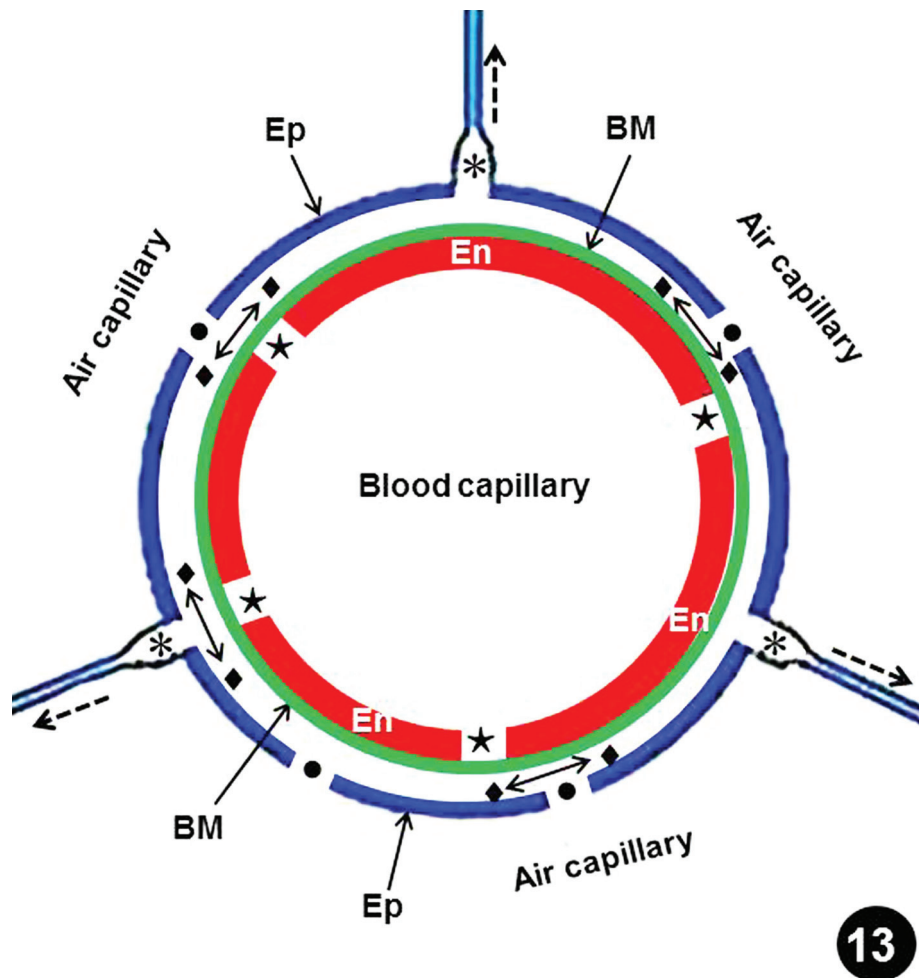


Figure 13. Drawing illustrating the presumptive process of the failure of the blood-gas barrier (BGB) of the blood-gas barrier breaks and the epithelial-epithelial cells connections breaks in the lung of the free range chicken, *Gallus gallus* variant *domesticus*. As the intramural pressures were increases, the endothelial cells separate at the intercellular junction (stars), allowing the blood plasma to leak out. The fluid percolates through the basement membrane (BM) and seeps to occupy the space between it and the epithelial cell (diamonds and double sided arrows). The tension of the blood capillary and the accumulation of fluid under the epithelial cell cause the epithelial-epithelial cells connections (E-ECCs) (dashed arrow) to separate (asterisks) and eventually fail. The E-ECCs may also fail from accumulation of blood and/or blood plasma in the air capillary after complete failure of the BGB. Dots, epithelial cell breaks.

The E-ECCs are the parts of the exchange tissue where epithelial cells separate adjacent ACs while connecting the BCs (Fig. 14). The epithelial cells are coupled back-to-back across a very thin basement membrane⁴⁰: these parts are not designed for load bearing. The pressures in the ACs are equal and the respiratory gases transfer by diffusion.³⁹ The load-bearing capacity of the BGB stems directly from its relatively greater thickness (compared to the E-ECCs) and presence of a distinctive basement membrane that contains type-IV collagen.⁴⁰ Depending on the extent of failure, blood plasma should initially ooze out leading blood to later flow out of the BCs into the ACs. The much heavier fluid should cause the delicate E-ECCs to stretch and eventually break. The close intertwining of the ACs and the BCs,^{4,5,41} which was described by West et al⁴² as ‘honeycomb arrangement’, creates contact interdependence which increases the strengths of the ACs and the BCs. Failure of 1 E-ECC from presence of blood plasma

and/or blood in an AC (after a break of the BGB) should set off a cascading process of failure of the E-ECCs as the fluid passes from 1 AC to another. The fact that the E-ECCs separate before the BGB fails shows that to an extent, these areas (the E-ECCs) strengthen the BGB. Employing the analogy of the spokes of a bicycle wheel, which are individually delicate but together support the wheel which in turn supports the weight of a rider, West et al⁴³ and West⁴⁴ postulated that the BCs are strengthened by the E-ECCs in the same manner. In the exchange tissue of the bird lung, the ACs and the BCs tolerate different forces (Fig. 14).

Birds in general lead highly energetic lifestyles.^{45,46} Compared to mammals, they have relatively high systemic blood pressures.¹² Systolic blood pressure as high as 400 mm Hg (53.3 kPa) has been reported in the turkey.⁴⁷ Termed ‘dissecting aneurism’ or ‘turkey heart attack’, fast growing healthy turkeys, *Meleagris gallopavo* (mostly males of between ages of

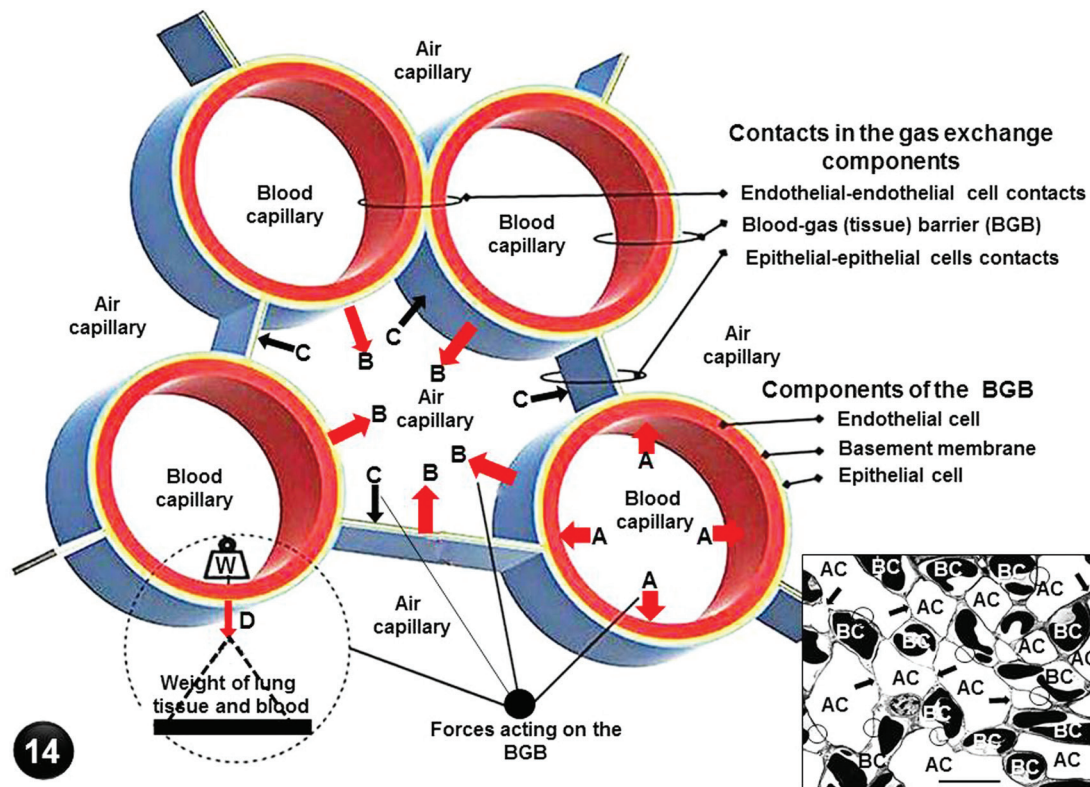


Figure 14. Diagram showing the forces which act on the blood-gas barrier (BGB) and the epithelial-epithelial cells connections (E-ECCs) in the exchange tissue of the avian lung. **A:** Blood in the blood capillaries is under pressure from the contractions of the heart muscle. The outward push creates circumferential tension which acts directly on the BGB and indirectly on the E-ECCs. **B:** Intermolecular forces at the air-water interface on the surfaces of the blood- and air capillaries produces surface tension which exerts an inward pull on the barrier. **C:** Intrapulmonary pressure exerts an outward push on the BGB and the E-ECCs. **D:** Depending on body posture, the weight (W) of lung tissue and blood contained in the blood capillaries tense the BGB. The insert shows the network of blood capillaries (BC) and air capillaries (AC) which form the gas exchange tissue of the lung. Circles, blood-gas barrier; arrows, epithelial-epithelial cell connections. Scale bar, 10 μm .

7 and 24 weeks), die suddenly of internal bleeding after aortic rupture.^{48–51} Compared to mammals, birds have larger hearts which comprise as much as 3% of their body mass¹³: with large stroke volumes and cardiac output (CO),⁴⁶ by extension, the pulmonary arterial- and the BC intramural pressures should also be relatively high in the bird lung. This was experimentally demonstrated by West et al,⁵² who by increasing the metabolic rate and the CO in anesthetized white leghorn breed of chickens by infusing them with 2,4 Dinitrophenol (DNP), a drug which uncouples oxidative phosphorylation and causes substantial increase in CO comparable to that during intense exercise, observed that the PA pressure increased steadily as CO increased. In an earlier study, in the duck, Geiser et al⁵³ had successfully used the same method (drug) to study the effects of increased metabolism on pulmonary gas exchange. As speculated by West et al,⁵² during strenuous activities like flight, the pulmonary artery blood pressure and by extension the transmural blood capillary pressure should increase greatly. Seeing that the designs of the BGBs of the avian- and mammalian lungs are fundamentally similar,^{3,8,10,21} it is paradoxical how the relatively thin BGB of the bird lung^{9,11,21} copes with high capillary intramural pressure. In this study,

it was observed that separation of the E-ECCs commonly occurred at an intramural pressure of 2.90 kPa, while failure of the BGB followed at the higher one of 3.39 kPa. Compared to the transmural pressures at which the BGB in the rabbit-, the dog-, and the horse lungs failed,^{15,17–20} i.e., at ~5, ~10, and ~14 kPa respectively, the BGB of the chicken lung failed at relatively lower intramural pressure. While this may suggest that the BGB of the lung of the free range chicken is relatively weaker, for animals of different sizes and BGB thicknesses, such cursory comparison is wrong. It has been shown that the load-bearing part of a barrier is the basement membrane and not the epithelial- and endothelial cells.^{54–57} In the chicken lung, the basement membrane is 0.045 μm thick⁸ compared to much thicker membranes of 0.174, 0.319, and 0.386 μm respectively in the rabbit, the dog, and the horse lungs¹⁵: when the intramural pressure at which the BGB of the chicken lung failed is normalized with the thickness of the basement membrane, the tension at which failure occurs in the free range chicken is 2.8 times greater than that for the rabbit and the dog and 2.4 times that of the horse. Furthermore, assuming a pulmonary capillary radius of 5 μm for the animals, by Laplace's equation,⁵⁸ $P = T/r$, where P is the pressure, T is



the wall tension, and r the radius, and taking into account the transmural/intramural pressures at which the BGB failed in rabbit-, the dog- and the horse lungs¹⁵ (~5, ~10, and ~14 kPa, respectively) and the chicken (this study; 0.94 kPa), the wall tensions were respectively 153, 151, 180, and 376 N/m²: the BGB in chicken lung tolerated 2½ times the wall tension for the rabbit and the dog and 2 times that of the horse. This shows that for its thickness (specifically that of the basement membrane), the BGB of the chicken lung is substantially stronger. The strength of the BGB allows it to maintain its structural integrity even during extreme cardiopulmonary functions.^{39,59}

Presence of type-IV collagen in the basement membrane of the BGB of the chicken lung⁴⁰ may foremost contribute to its strength. Possible existence of a tensegrity (tension-integrity) state⁶⁰ in the exchange tissue of the avian lung was suggested by Maina.^{61–62} In the avian lung, the structural components, which should contribute to the tensegrity by creating continuous tension and discontinuous compression, are the smooth muscles and the elastic tissue fibers, which generate tension and collagen fibers, which then counter it.⁶³ In lungs of dead birds (like those investigated here), loss of the tone of the neurally-controlled smooth muscle components should remove the balance of forces, consequently eliminating tensegrity: the in-life strength of the BGB and the E-ECCs of the exchange tissue of avian lung cannot be directly studied on the lung of a dead bird. It is plausible that the transmural pressure at which the BGB in the lung of a living chicken fails is greater than that reported here.

Critique of the Methods

It is important to point out certain shortcomings in the techniques used in this study. These are listed below.

- a) Unlike the mammalian respiratory system, which can be perfused at known transpulmonary pressure, after inflating the lung and closing the only opening, the trachea,⁶⁴ the avian respiratory system cannot be handled that way. This is because damage of the disseminated air sacs is unavoidable when the coelomic cavity is opened to access the heart, cannulate the blood vessels, and perfuse the lungs. During the process, the cranial- and caudothoracic air sacs, which lie close to the heart, are particularly liable to damage. If these or any of the other air sacs are punctured, the intrapulmonary pressure is lost and with it the balance of forces across the BGB. Balancing of forces across the E-ECCs and the BGB during perfusion of the avian lung is then technically impossible.
- b) The hydrodynamics of the flow of the phosphate buffered saline (PBS) through the chicken lung, with the animal lying in a supine position, are not known. In the human lung, Nyren et al⁶⁵ observed that pulmonary perfusion is more uniform when a person is positioned in a prone- than a supine position. In the avian lung, the effect may be negligible because of its relative small

size, its rigidity, and its firm attachment to the vertebral column and the ribs.

- c) The PBS, which was used to perfuse the lung in this study, is a Newtonian fluid. This is in contrast to blood, which, with suspended cells like the white- and the red cells, is non Newtonian. In a pilot study that preceded this study, an attempt was made to collect and use autologous blood to perfuse the lung. It was, however, impossible to collect enough of it for meaningful perfusion. Furthermore, plasma expander (Dextran T70) was used to increase the viscosity of the PBS, but the results did not differ from those where only PBS was used.

Conclusion

Although the basement membrane of the BGB of the avian lung is relatively thinner than that of some mammals for which comparable data are available, i.e., the rabbit, the dog, and the horse, it appears be relatively stronger. Strong BGB may explain how birds cope with high cardiovascular blood pressures, which should translate into high pulmonary arterial- and capillary intramural blood pressures. In birds, strong BGB supports high energetic lifestyles. A number of factors explain the strength of the BGB. These are that a) the basement membrane contains the especially strong type-IV collagen,¹⁶ b) in the manner of the spokes of a bicycle wheel, the BCs are suspended by the E-ECCs,^{43,44} and c) the presence of contractile- (smooth muscle and elastic tissue) and non-contractile (collagen) tissue components⁶³ imparts a state of tensegrity, which strengthens the BGB.^{62,64} In the poultry industry, annual losses from rupture of the heart and the blood vessels run into billions of dollars.⁶⁶ In turkeys, mortalities from aortic rupture of between 20% and 43.7% were reported by Simpson⁶⁵ and Krista et al.⁶⁶ Pulmonary hypertension may indirectly lead to these complications.^{67,68} Losses in the commercial poultry industry are regrettable because compared to, e.g., beef, as a source of animal protein to the increasing human population, poultry meat continues to be the more affordable alternative. Understanding the pathogenesis of the BGB failure may help in the formulation of husbandry practices, which reduce economic losses.

Acknowledgements

The authors would like to thank Patrick Selahle and Mary Ann of the Central Animal Service (CAS) Unit of the University of the Witwatersrand for procurement and husbandry of the birds. Ms Pamela Sharp provided excellent technical assistance with electron microscopy.

Author Contributions

Conceived and designed the experiments: JNM, SAJ. Wrote the first draft of the manuscript: SAJ. Revised and improved the manuscript JNM. Agreed with results and conclusions: JNM, SAJ. Submitted the manuscript: JNM. All authors reviewed and approved of the final manuscript.



DISCLOSURES AND ETHICS

As a requirement of publication the authors have provided signed confirmation of their compliance with ethical and legal obligations including but not limited to compliance with ICMJE authorship and competing interests guidelines, that the article is neither under consideration for publication nor published elsewhere, of their compliance with legal and ethical guidelines concerning human and animal research participants (if applicable), and that permission has been obtained for reproduction of any copyrighted material. This article was subject to blind, independent, expert peer review. The reviewers reported no competing interests.

REFERENCES

1. Duncker HR. The lung air sac system of birds. A contribution to the functional anatomy of the respiratory apparatus. *Ergeb Anat Entwicklungsgesch.* 1971;45:1–171.
2. McLelland J. *Anatomy of the lungs and air sacs, in Form and Function in Birds, Vol. 4.* London: Academic Press; 221–279.
3. Maina JN. *The Lung-Air Sac System of Birds: Development, Structure, and Function.* 2005; Heidelberg: Springer-Verlag.
4. Woodward JD, Maina JN. A 3D digital reconstruction of the components of the gas exchange tissue of the lung of the muscovy duck, *Cairinoschata*. *J Anat.* 2005;206(5):477–492.
5. Woodward JD, Maina JN. Study of the structure of the air and blood capillaries of the gas exchange tissue of the avian lung by serial section three-dimensional reconstruction. *J Microsc.* 2008;230(Pt 1):84–93.
6. Macklem PT, Bouverot P, Scheid P. Measurement of the distensibility of the parabronchi in duck lungs. *Respir Physiol.* 1979;38(1):23–35.
7. Powell FL, Hastings RH, Mazzone RW. Pulmonary vascular resistance during unilateral pulmonary arterial occlusion in ducks. *Am J Physiol.* 1985;249(1 Pt 2):R39–R43.
8. Watson RR, Fu Z, West JB. Minimal distensibility of pulmonary capillaries in avian lungs compared with mammalian lungs. *Respir Physiol Neurobiol.* 2008;160(2):208–214.
9. Watson RR, Fu Z, West JB. Morphometry of the extremely thin pulmonary blood-gas barrier in the chicken lung. *Am J Physiol Lung Cell Mol Physiol.* 2007;292(3):L769–L777.
10. Gehr P, Mwangi DK, Amman A, Maloij GMO, Taylor CR, Weibel ER. Design of the mammalian respiratory system. V. Scaling morphometric pulmonary diffusing capacity to body mass: wild and domestic animals. *Respiration Physiology.* 1981;44:61–86.
11. Maina JN, King AS, Settle G. An allometric study of pulmonary morphometric parameters in birds, with mammalian comparisons. *Philos Trans R Soc Lond B Biol Sci.* 1989;326(1231):1–57.
12. Seymour RS, Blaylock AJ. The principle of Laplace and scaling of ventricular wall stress and blood pressure in mammals and birds. *Physiol Biochem Zool.* 2000;73(4):389–405.
13. Hartmann FA. Heart weight in birds. *Condor.* 1955;57:221–238.
14. Berger M, Hart JS, Roy OZ. Respiratory water and heat loss of the black duck during flight at different ambient temperatures. *Can J Zool.* 1971;49(5):767–774.
15. Birks EK, Mathieu-Costello O, Fu Z, Tyler WS, West JB. Comparative aspects of the strength of pulmonary capillaries in rabbit, dog, and horse. *Respir Physiol.* 1994;97(2):235–246.
16. Maina JN, Jimoh SA. Structural failures of the blood-gas barrier and the epithelial-epithelial cell connections in the different vascular regions of the lung of the domestic fowl, *Gallus gallus* variant domesticus, at rest and during exercise. *Biol Open.* 2013;2(3):267–276.
17. West JB, Tsukimoto K, Mathieu-Costello O, Prediletto R. Stress failure in pulmonary capillaries. *J Appl Physiol.* 1991;70:1731–1742.
18. West JB, Mathieu-Costello O. Strength of the pulmonary blood-gas barrier. *Respir Physiol.* 1992;88(1–2):141–148.
19. West JB, Mathieu-Costello O, Jones JH, et al. Stress failure of pulmonary capillaries in racehorses with exercise-induced pulmonary hemorrhage. *J Appl Physiol (1985).* 1993;75(3):1097–1109.
20. Mathieu-Costello O, Willford DC, Fu Z, Garden RM, West JB. Pulmonary capillaries are more resistant to stress failure in dogs than in rabbits. *J Appl Physiol (1985).* 1995;79(3):908–917.
21. Maina JN, West JB. Thin and strong! The bioengineering dilemma in the structural and functional design of the blood-gas barrier. *Physiol Rev.* 2005; 85(3):811–844.
22. Bhattacharya J, Nanjo S, Staub NC. Micropuncture measurement of lung microvascular pressure during 5-HT infusion. *J Appl Physiol Respir Environ Exerc Physiol.* 1982;52(3):634–637.
23. West JB. *Respiratory Physiology: The Essentials, 8th Edition.* 2008; Baltimore: Lippincott and Wilkins.
24. Feld J, Carper KL. *Construction Failure.* 1997; New York: John Wiley and Sons.
25. Stephens RI, Fuchs HO (Eds.). *Metal Fatigue in Engineering (2nd Edition).* 2001; New York: John Wiley and Sons.
26. Li J, Connell S, Shi R. Biomimetic architectures for tissue engineering. In Murkajee A, Ed. *Biomimetics, Learning from Nature.* 2010; Rijeka: InTech; 488–505.
27. Whipp BJ, Ward SA. Cardiopulmonary coupling during exercise. *J Exp Biol.* 1982;100:175–193.
28. Turner DL. Cardiovascular and respiratory control mechanisms during exercise: an integrated view. *J Exp Biol.* 1991;160:309–340.
29. Raven PB, Potts JT. Cardiovascular responses to exercise and training. In Harries M, Williams C, Stanish WD, Micheli E (Eds). *Oxford Textbook of Sport Medicine, 2nd Edition.* 2000; New York: Oxford University Press.
30. Thomas DP, Fregin GF. Cardiorespiratory and metabolic responses to treadmill exercise in the horse. *J Appl Physiol Respir Environ Exerc Physiol.* 1981; 50(4):864–868.
31. Bamford OS, Maloij GM. Energy metabolism and heart rate during treadmill exercise in the Marabou stork. *J Appl Physiol Respir Environ Exerc Physiol.* 1980;49(3):491–496.
32. Hart JS, and Roy OZ. Respiratory and cardiac responses to flight in pigeons. *Physiological Zoology.* 1966;39:291–305.
33. Zhixiang T, Xinqiao J. Biomaterial-based strategies for the engineering of mechanically active soft tissues. *MRS Communications.* 2012;2:31–39.
34. Schoene RB, Hackett PH, Henderson WR, et al. High-altitude pulmonary edema. Characteristics of lung lavage fluid. *JAMA.* 1986;256(1):63–69.
35. Hopkins SR, Schoene RB, Henderson WR, Spragg RG, Martin TR, West JB. Intense exercise impairs the integrity of the pulmonary blood-gas barrier in elite athletes. *Am J Respir Crit Care Med.* 1997;155(3):1090–1094.
36. Abdalla MA, King AS. The functional anatomy of the pulmonary circulation of the domestic fowl. *Respir Physiol.* 1975;23(3):267–290.
37. Abdalla MA, King AS. Pulmonary arteriovenous anastomoses in the avian lung: do they exist? *Respir Physiol.* 1976;27(2):187–191.
38. Abdalla MA. The blood supply to the lung. In King AS, McLelland J, Eds. *Form and Function in Birds, Volume 4.* 1989; London: Academic Press; 281–306.
39. Powell FL. *Respiration.* In Whitton GC, Ed. *Sturkie's Avian Physiology, 5th Edition.* 2000; New York: Academic Press; 233–259.
40. Jimoh SA, Maina JN. Immuno-localization of type-IV collagen in the blood-gas barrier and the epithelial-epithelial cell connections of the avian lung. *Biol Lett.* 2013;9(1):20120951.
41. Maina JN, Woodward JD. Three-dimensional serial section computer reconstruction of the arrangement of the structural components of the parabronchus of the Ostrich, *Struthiocamelus* lung. *Anat Rec (Hoboken).* 2009;292(11):1685–1698.
42. West JB, Watson RR, Fu Z. Major differences in the pulmonary circulation between birds and mammals. *Respir Physiol Neurobiol.* 2007;157(2–3):382–390.
43. West JB, Watson RR, Fu Z. The human lung: did evolution get it wrong? *Eur Respir J.* 2007;29(1):11–17.
44. West JB. Comparative physiology of the pulmonary blood-gas barrier: the unique avian solution. *Am J Physiol Regul Integr Comp Physiol.* 2009;297(6): R1625–R1634.
45. Tucker VA. Metabolism during flight in the laughing gull, *Larus atricilla*. *Am J Physiol.* 1972;222(2):237–245.
46. Butler PJ. Exercise in birds. *Journal of Experimental Biology.* 1991;160:233–262.
47. Carsten J, Labrosse MR, Thubrikar MJ, Robicsek F. Role of aortic root motion in the pathogenesis of aortic dissection. *Circulation.* 2004;109:763–769.
48. Collins JJ. Dissecting aneurysms in turkeys and man. *Arch Surg.* 1971;102(2): 159–160.
49. Neumann F, Ungar H. Spontaneous aortic rupture in turkeys and the vascularization of the aortic wall. *Can Vet J.* 1973;14(6):136–138.
50. Krista LM, Beckett SD, McDaniel GR, Patterson RM, Mora EC. Rupture pressure of elastic and muscular aortic segments from hypertensive and hypotensive turkeys. *Br Poult Sci.* 1986;27(2):207–213.
51. van Veen L. [Aortic rupture in poultry: a review]. *Tijdschr Diergeneesk.* 1999; 124(8):244–247. Dutch.
52. West JB, Fu Z, Gu Y, Wagner HE, Carr JA, Peterson KL. Pulmonary artery pressure responses to increased cardiac output in chickens with raised metabolic rate. *Comp Biochem Physiol A Mol Integr Physiol.* 2010;156:430–435.
53. Geiser J, Gratz RK, Hiramoto T, Scheid P. Effects of increased metabolism by 2,4-dinitrophenol on respiration and pulmonary gas exchange in the duck. *Respir Physiol.* 1984;57:1–14.
54. Williamson JR, Vogler NJ, Kilo C. Regional variations in the width of the basement membrane of muscle capillaries in man and giraffe. *Am J Pathol.* 1971; 63(2):359–370.
55. Welling LW, Grantham JJ. Physical properties of isolated perfused renal tubules and tubular basement membranes. *J Clin Invest.* 1972;51(5):1063–1075.
56. Haworth SG, Hall SM, Panja M, Patel M. Peripheral pulmonary vascular and airway abnormalities in adolescents with rheumatic mitral stenosis. *Int J Cardiol.* 1988;18(3):405–416.
57. Swayne GT, Smaje LH, Bergel DH. Distensibility of single capillaries and venules in the rat and frog mesentery. *Int J Microcirc Clin Exp.* 1989;8(1):25–42.



58. Valentinuzzi ME, Kohen AJ, Zanutto BS. Laplace's law. Its epistemological context. *IEEE Pulse*. 2011;2(6):71–76.
59. Peters GW, Steiner DA, Rigoni JA, Mascilli AD, Schnepf RW, Thomas SP. Cardiorespiratory adjustments of homing pigeons to steady wind tunnel flight. *J Exp Biol*. 2005;208(Pt 16):3109–3120.
60. Ingber DE. The architecture of life. *Scientific American*. 1998;278:18–57.
61. Maina JN. Minutialization at its extreme best! The underpinnings of the remarkable strengths of the air and the blood capillaries of the avian lung: a conundrum. *Respir Physiol Neurobiol*. 2007;159(2):141–5; author reply 146.
62. Maina JN. Spectacularly robust! Tensegrity principle explains the mechanical strength of the avian lung. *Respir Physiol Neurobiol*. 2007;155(1):1–10.
63. Maina JN, Jimoh SA, Hosie M. Implicit mechanistic role of the collagen, smooth muscle, and elastic tissue components in strengthening the air and blood capillaries of the avian lung. *J Anat*. 2010;217(5):597–608.
64. Fu Z, Costello ML, Tsukimoto K, et al. High lung volume increases stress failure in pulmonary capillaries. *J Appl Physiol (1985)*. 1992;73(1):123–133.
65. Nyrén S, Mure M, Jacobsson H, Larsson SA, Lindahl SG. Pulmonary perfusion is more uniform in the prone than in the supine position: scintigraphy in healthy humans. *J Appl Physiol (1985)*. 1999;86(4):1135–1141.
66. Currie RJ. Ascites in poultry: recent investigations. *Avian Pathol*. 1999;28(4):313–326.
67. Simpson CF. Relation of hemodynamics to the incidence of diethylstilbestrol-induced aortic ruptures in hypertensive and hypotensive lines of turkeys. *Atherosclerosis*. 1978;30(4):249–254.
68. Krista LM, Waibel PE, Shoffner RN, Sautter JH. Natural dissecting aneurysm (aortic rupture) and blood pressure in the turkey. *Nature*. 1967;214(5093):1162–1163.